Impact of membrane bistability on dynamical response of neuronal populations

Wei Wei,[1,2,*] Fred Wolf,[3] and Xiao-Jing Wang[1,2,4]

[1]*Center for Neural Science, New York University, New York, New York 10003, USA*

[2]*Department of Neurobiology and Kavli Institute for Neuroscience, Yale University School of Medicine, New Haven, Connecticut 06520, USA*

[3]*Max Planck Institute for Dynamics and Self-Organization and Bernstein Center for Computational Neuroscience, D-37077 Göttingen, Germany*

[4]*NYU-ECNU Institute of Brain and Cognitive Science, NYU Shanghai, Shanghai, China*

(Received 5 January 2015; revised manuscript received 5 August 2015; published 25 September 2015)

Neurons in many brain areas can develop a pronounced depolarized state of membrane potential (up state) in addition to the normal hyperpolarized state near the resting potential. The influence of the up state on signal encoding, however, is not well investigated. Here we construct a one-dimensional bistable neuron model and calculate the linear dynamical response to noisy oscillatory inputs analytically. We find that with the appearance of an up state, the transmission function is enhanced by the emergence of a local maximum at some optimal frequency and the phase lag relative to the input signal is reduced. We characterize the dependence of the enhancement of frequency response on intrinsic dynamics and on the occupancy of the up state.

DOI: 10.1103/PhysRevE.92.032726 PACS number(s): 87.19.ll, 05.40.−a, 87.19.ls

I. INTRODUCTION

The elevated state of the neuronal membrane potential (MP), the so-called up state, has been observed extensively in different brain areas [1–9]. In this regime the MPs of neurons are characterized by a bimodal distribution resulting from two stable fixed points in membrane dynamics. This bistability of neuronal dynamics leads to synchronous transitions between the down and up states of neurons in a network and the development of global up and down states [10,11]. The exact role of the bistability of MP in signal encoding and processing is still not well understood.

Individual neurons in a network receive noisy synaptic inputs and fire spikes irregularly [12]. Besides the stationary firing rate, one important characteristic of neuronal dynamics is the response to time varying signals superimposed on background noise [13,14]. This dynamical response of cortical neurons has recently been measured experimentally up to 1 kHz of signal frequency, which revealed very high cutoff frequencies [15–19]. Theoretically, the linear dynamical response has been obtained analytically for the leaky integrate-and-fire (LIF) neuron [20,21], in which membrane dynamics has only one stable fixed point, and for the $r-\tau$ model (a piecewise linear version of the exponential integrate-and-fire model) [22], in which an additional unstable fixed point for action potential initiation was included. The effect of the unstable fixed point in membrane dynamics on dynamical response was also investigated numerically in other one-dimensional models and conductance-based models [23–27]. A theoretical characterization of the dynamical response of neurons that exhibit up and down states, however, is still missing. Intuitively, when the membrane potential of a neuron has a higher probability to be around some depolarized voltage, it is more likely that a small oscillatory signal can contribute to the firing of spikes, leading to enhancement of frequency response. Here we propose an analytically solvable bistable neuron model to investigate the impact of the up state on the dynamical response of neurons.

II. MODEL DESCRIPTION

In this work we construct a one-dimensional bistable neuron model, which has piecewise linear subthreshold dynamics and is analytically solvable for the linear dynamical response. The dynamics is described by the following Langevin equation:

$$\tau\dot{v} = f(v) + \mu + \sigma\eta(t)\,, \tag{1}$$

where

$$f(v) = \begin{cases} -v, & -\infty < v \leqslant v_0 \\ r_1(v - v_{t1}), & v_0 < v \leqslant v_1 \\ r(v - v_{t0}), & v_1 < v \leqslant v_b. \end{cases} \tag{2}$$

Here τ is the membrane time constant near the resting potential, v is the MP relative to the resting potential, μ is the mean external input, $\eta(t)$ is a Gaussian white noise which satisfies $\langle\eta(t)\rangle = 0$ and $\langle\eta(t)\eta(t')\rangle = \tau\delta(t-t')$, and σ is the strength of the noise. We will take τ as the unit of time in the theoretical results. Note that the membrane dynamics here might result from an interaction between patterned synaptic inputs and intrinsic membrane dynamics. Figure 1(a) shows an illustration of the model dynamics when there is no external input. The slopes of the middle and right pieces are denoted as r_1 and r, respectively. Note that r characterizes the membrane dynamics around the higher stable fixed point where the time constant is given by $\tau/|r|$. MPs at the crossing points of the left piece with the middle piece, and the middle piece with the right piece are denoted as v_0 and v_1, respectively. When there is no external input, v_{t1} and v_{t0} are the unstable fixed point and the higher stable fixed point, respectively. We will fix v_0 and v_{t0}, whereas v_{t1} and v_1 are given by $v_{t1} = (1 + 1/r_1)v_0$ and $v_1 = (r_1 v_{t1} - r v_{t0})/(r_1 - r)$. The deterministic dynamics [$\sigma = 0$ in Eq. (1)] possess one lower stable fixed point, one unstable fixed point, and one higher stable fixed point, located at $v = \mu$, $v_{t1} - \mu/r_1$, and $v_{t0} - \mu/r$, respectively. When the MP reaches an absorbing boundary v_b, it is reset to a resetting potential v_r for a refractory period τ_r. The larger

*ww41@nyu.edu

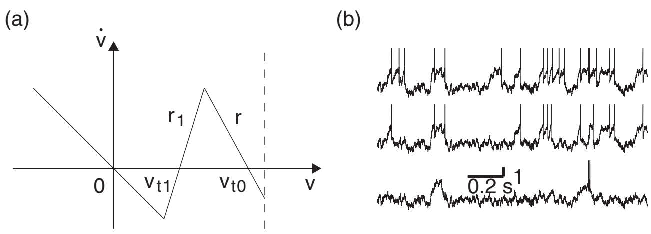

FIG. 1. Illustration of the model. (a): illustration of the piecewise linear model; (b): MP trajectories for $r_1 = 1$, 5, and 10 from bottom to top. Parameters used are: $r = -1$, $v_0 = 0.5$, $v_r = v_{t1}$, $v_{t0} = 2$, $\tilde{v}_b = -0.2$, $\tau = 10$ ms, $\tau_r = 0$ ms, $\mu = 0$, $\sigma = 0.5$.

one between $|\tilde{v}_0|$ and $|\tilde{v}_b|$ determines the rheobase current of the model neuron, where $\tilde{v}_0 \equiv -v_0$ and $\tilde{v}_b \equiv r(v_b - v_{t0})$. Since the model neuron will never fire spikes when $|r|$ is very large if v_b is fixed, we will fix $\tilde{v}_b$ and choose v_b determined by $v_b = v_{t0} + \tilde{v}_b/r$. The relative values of $\tilde{v}_0$ and $\tilde{v}_b$ might indicate different dynamical regimes of the model neuron. For example, a larger $|\tilde{v}_b|$ implies that the neuron can make a transition from the up-down regime to a tonically depolarized state when $\mu > |\tilde{v}_0|$, which is reminiscent to that observed for cortical neurons from sleep to wakefulness [28]. We are most interested in the noise-driven regime, i.e., the mean external current is smaller than the rheobase current, since real neurons work in a regime in which excitatory and inhibitory synaptic inputs to individual neurons balance each other [29]. In this dynamic regime, our neuron model describes barrier penetration in a double well with reinjection of probability current after reaching an absorbing boundary. Here we focus on the case when v_r is located within the middle piece, therefore the model neuron could fire several spikes before transiting to the down state, as normally observed for neurons exhibiting up and down states. Figure 1(b) shows the MP trajectories for three different r_1. We see that with a larger r_1, the MP spends more times at the up state.

III. THE FOKKER-PLANCK EQUATION (FPE) FRAMEWORK

The FPE corresponding to Eq. (1) has the following form [30]:

$$\partial_t P(v,t) + \partial_v[f(v) + \mu - D\partial_v]P(v,t) = 0 \, , \tag{3}$$

where $D = \frac{1}{2}\sigma^2$ is the diffusion constant. We will use both D and σ in the following. Defining the probability current as $J(v,t) = [f(v) + \mu - D\partial_v]P(v,t)$, the FPE then becomes the equation for probability conservation, $\partial_t P(v,t) + \partial_v J(v,t) = 0$.

The boundary conditions are specified in the following (subscripts 1, 2, 3 indicate the left, right, and middle MP regions in Fig. 1(a). At the absorbing boundary v_b, $P_2(v_b,t) = 0$. At the resetting point v_r, $P_3(v_r^+,t) - P_3(v_r^-,t) = 0$, and $\partial_v P_3(v_r^+,t) - \partial_v P_3(v_r^-,t) = \partial_v P_2(v_b, t - \tau_r)$, from the resetting condition and continuity of the probability density and probability current. At v_0 and v_1, the probability density and its derivative are continuous: $P_1(v_0,t) = P_3(v_0,t)$, $\partial_v P_1(v_0,t) = \partial_v P_3(v_0,t)$, $P_3(v_1,t) = P_2(v_1,t)$, and $\partial_v P_3(v_1,t) = \partial_v P_2(v_1,t)$. Finally the normalization condition of the probability density requires $\lim_{v\to-\infty} P_1(v,t) = 0$. With these boundary conditions the asymptotic solution of the FPE is uniquely determined (the possible transient is not of interest here). The instantaneous firing rate is given by the probability current through the absorbing boundary, $\nu(t) \equiv J(v_b,t) = -D\partial_v P_2(v_b,t)$.

IV. DEVELOPMENT OF THE UP STATE

When the mean input to a model neuron is constant, the stationary probability density, denoted as $P_0(v)$, can be obtained by setting $J(v,t) = \nu_0$, where ν_0 is the stationary firing rate and is determined by the normalization condition of the stationary density, $\int_{-\infty}^{v_b} P_0(v)\, dv = 1$ [see Appendix A for the expressions of $P_0(v)$ and ν_0]. The existence of the up state requires the appearance of a local maximum of the probability density at a depolarized MP value. Two peaks appear in $P_0(v)$ if there exists an up state in the MP trajectories, located around the lower stable fixed point and the higher stable fixed point, which will be denoted as P_0^{down} and P_0^{up}, respectively. The MPs corresponding to the two peaks, denoted as v_{down} and v_{up}, are the mean values of MPs at the down state and up state, respectively. From the expression of $P_0(v)$, it is easy to see that the down state locates at the lower stable fixed point, $v_{\text{down}} = \mu$. The development of a local maximum

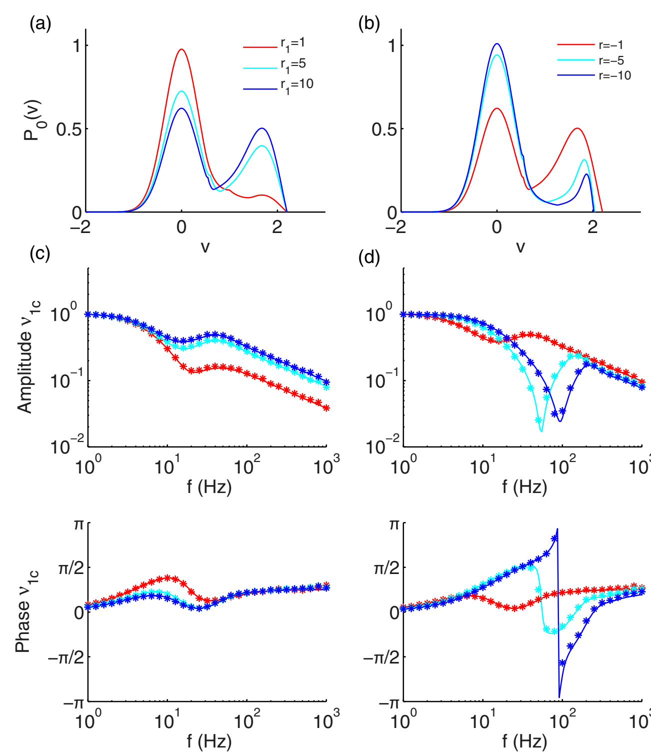

FIG. 2. (Color online) Dependence of stationary probability density and linear dynamical response on r_1 and r. (a) and (b): probability density for different r_1 and r. (c) and (d): dependence of the transmission function (upper panels) and phase lag (lower panels) of the linear dynamical response on r_1 and r. The linear dynamical response is normalized with the value at $f = 1$ Hz. Signal frequency f is related to the angular frequency ω by $\omega = 2\pi f$. Solid lines are from theoretical results and asterisks are from simulations. Parameters used: $r = -1$ in (a) and (c), $r_1 = 10$ in (b) and (d). Other parameters are the same as in Fig. 1.

around the higher stable fixed point requires $P'_{02}(v) = 0$ since the probability density decreases monotonically when $0 < v < v_1$, or equivalently, the following equation:

$$x e^{-x^2} \int_{x_b}^{x} e^{x'^2}\, dx' = \frac{1}{2} \tag{4}$$

has a solution within the range $v_1 < v < v_b$, where $x \equiv \frac{r(v-v_{t0})+\mu}{\sqrt{-r\sigma}}$, $x_b \equiv \frac{r(v_b-v_{t0})+\mu}{\sqrt{-r\sigma}}$, with $v_{\rm up}$ independent of r_1. Since $x_b < x$, we have $x > 0$ and $v_1 < v_{\rm up} < v_{t0} - \mu/r$ from Eq. (4). Therefore the mean value of the MP at the up state locates lower than the higher stable fixed point in the deterministic dynamics due to the influence of noise and the absorbing boundary. The probability density at $v = v_{\rm up}$ is given by

$$P_0^{\rm up} = \frac{\nu_0}{r(v_{\rm up} - v_{t0}) + \mu}\ . \tag{5}$$

The dependence of $P_0(v)$ on r_1 and r is shown in Figs. 2(a) and 2(b). With the increase of r_1, the transition from the up state to the down state becomes more difficult, therefore the MP resides on the up state for a longer time [Fig. 1(b)], indicating a larger ratio between the maximal probability density at the up state and down state [Fig. 2(a)]. Note that changing the slope r_1 can determine whether the up state exists or not by adjusting v_1, but does not influence the position of $v_{\rm up}$ if it exists. With the increase of $|r|$ (the absolute value of r), $v_{\rm up}$ is shifted slightly towards the higher deterministic fixed point and the ratio $P_0^{\rm up}/P_0^{\rm down}$ decreases [Fig. 2(b)].

V. LINEAR DYNAMICAL RESPONSE

Now consider a weak sinusoidal signal encoded in the mean input, $\mu(t) = \mu + \varepsilon\cos(\omega t)$, where ε is small. At the linear order in ε, the instantaneous firing rate is given by $\nu(t) = \nu_0 + \varepsilon|\nu_{1c}(\omega)|\cos[\omega t - \phi_c(\omega)]$, where $|\nu_{1c}(\omega)|$ is the transmission function and $\phi_c(\omega)$ is the phase lag. We find that a complex response function $\nu_{1c}(\omega)$ can be obtained analytically by solving the FPE at the linear order using the Green's function method. The transmission function is the absolute value of $\nu_{1c}(\omega)$, while the phase lag $\phi_c(\omega)$ is given by the phase angle, $\phi_c(\omega) = \arg[\nu_{1c}(\omega)]$. The expression of $\nu_{1c}(\omega)$ reads

$$\begin{aligned}\nu_{1c}(\omega) = \frac{1}{B}\Bigg[&\frac{i\omega(1+1/r_1)}{(1-i\omega)(1+i\omega/r_1)}(\psi_1 P_{01} - \sqrt{D}\Phi_1 P'_{01}) + \frac{i\omega(1/r_1 - 1/r)}{(1+i\omega/r)(1+i\omega/r_1)}(\psi_1 Y'_5 - \psi'_1 Y_5)P_{02}(v_1)\, e^{\Delta_1}\\ &+ \frac{\sqrt{Dr_1}(r-r_1)}{(r_1+i\omega)(r+i\omega)}(\psi_1 Y'_{51} - \psi'_1 Y_{51})P'_{02}(v_1)\, e^{\Delta_1} + \frac{\nu_0/\sqrt{Dr_1}}{1+i\omega/r_1}(\psi_1 Y'_{51r} - \psi'_1 Y_{51r})e^{\Delta_0}\\ &- \frac{\nu_0/\sqrt{D|r|}}{1+i\omega/r}[(\psi_1 Y'_5 - \psi'_1 Y_5)Y'_2 - (\psi_1 Y'_6 - \psi'_1 Y_6)Y_2]e^{\Delta_2}\Bigg],\end{aligned} \tag{6}$$

where $\psi_1(v)$, $\Phi_1(v)$, etc., are parabolic cylinder functions [31], and $Y_1(v)$, $Y_5(v)$, B, etc., are combinations of them to simplify the expression, as defined in Appendix B. Note the functions adopt their values at $v = v_0$, unless denoted otherwise. Taking $\omega \to \infty$ in Eq. (6), we find that the high frequency limit is the same as the LIF model and the $r-\tau$ model, i.e., $\nu_{1c} \to \frac{\nu_0}{\sqrt{D}}\frac{1}{\sqrt{\omega}}\, e^{i\frac{\pi}{4}}$. This high frequency limit is characteristic of the linear sub-threshold dynamics and absorbing boundary [22].

VI. FREQUENCY-SELECTIVE ENHANCEMENT OF LINEAR DYNAMICAL RESPONSE BY THE UP STATE

The dependence of the linear dynamical response on r_1 and r are shown in Figs. 2(c) and 2(d). We see that a local maximum of the transmission function, denoted as $\nu_{1c}^{\max}$, appears at frequency $f^{\max}$ [Figs. 2(c) and 2(d), upper panels] accompanying the development of the up state [Figs. 2(a) and 2(b)]. The local maximal value of the transmission function at the resonance frequency increases with r_1 and decreases with $|r|$, following the same trend as the ratio between the probability density at $v_{\rm up}$ and $v_{\rm down}$ [Figs. 2(a) and 2(b)]. The phase lag of the firing rate response relative to the input signal is reduced when there is a more pronounced up state [Figs. 2(c) and 2(d), lower panels]. Therefore the up state can enhance the dynamical response by developing local maximum at some specific resonance frequency, and reduce the phase lag of the response.

We characterize the relationship between the up state occupancy and resonance in the linear dynamical response quantitatively in Fig. 3. While the ratio between probability densities at $v_{\rm up}$ and $v_{\rm down}$ increases with r_1 [Fig. 3(a)], the maximal value of the transmission function at the resonance frequency also increases with r_1 [Fig. 3(c)]. This leads to an increase of $\nu_{1c}^{\max}$ with $P_0^{\rm up}/P_0^{\rm down}$ [Fig. 3(c), inset]. Similarly, $\nu_{1c}^{\max}$ decreases with $|r|$ [Fig. 3(d)], following with the same trend as $P_0^{\rm up}/P_0^{\rm down}$ except for an initial small $|r|$ regime where there is no local maximum for $|\nu_{1c}(\omega)|$ [Fig. 3(b)]. This also leads to an increase of $\nu_{1c}^{\max}$ with $P_0^{\rm up}/P_0^{\rm down}$ [Fig. 3(d), inset]. The signal frequency at which the transmission function is maximally enhanced, $f^{\max}$, keeps constant when r_1 increases, i.e., being independent of the time scale characterizing the transition between up and down states [Fig. 3(e)]. On the contrary, $f^{\max}$ goes to higher frequencies when $|r|$ increases [Fig. 3(f)], and therefore is determined by the membrane time constant at the up state, $\tau/|r|$.

We tested the predication by using a neuron model with biophysically realistic membrane currents, which includes a non-inactivating potassium current controlling the up state and an inward rectifying potassium current stabilizing the down state [11]. We find that the normalized frequency response is strongly enhanced with the development of the up state (see Appendix C).

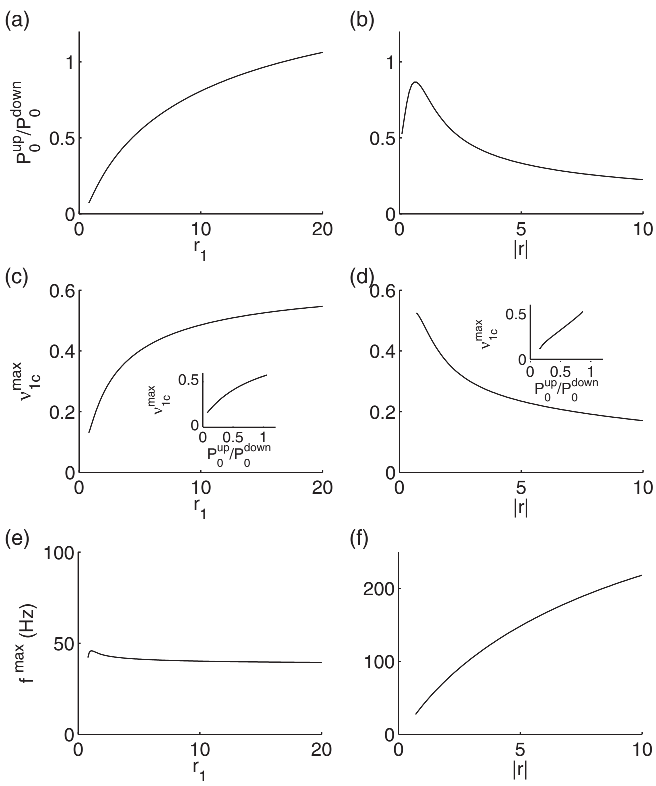

FIG. 3. Dependence of up state occupancy and resonance in the linear dynamical response on r_1 and r. (a) and (b): the up state occupancy $P_0^{\rm up}/P_0^{\rm down}$ as a function of r_1 (a) and $|r|$ (b). (c) and (d): the local maximal value $\upsilon_{1c}^{\rm max}$ of the normalized transmission function as a function of r_1 (c) and $|r|$ (d). Insets: $\upsilon_{1c}^{\rm max}$ as a function of $P_0^{\rm up}/P_0^{\rm down}$ due to the change of r_1 (c) and $|r|$ (d). (e) and (f): the resonance frequency $f^{\rm max}$ as a function of r_1 (e) and $|r|$ (f). Parameters used: $r = -1$ in (a) and $r_1 = 10$ in (b). Other parameters are the same as in Fig. 1.

VII. DISCUSSION

Dynamical response to noisy oscillatory inputs is a fundamental characterization of neurons' capability in signal encoding and transmission. Our model predicts a frequency-selective enhancement of signal transmission with the development of the up state. This prediction can be experimentally tested for neurons exhibiting up and down states by performing experiments similar to that in [15]. Selective enhancements of specific high frequency components of signals might be functionally beneficial for neural communication, since signals with frequencies within the γ band (30–100 Hz) or "high gamma" (>100 Hz) have been suggested to synchronize inter-regional brain activity [32–34]. Firing reliability of bistable neurons driven by time-dependent inputs were investigated numerically in the Morris-Lecar model [35]. Bistable piecewise linear membrane dynamics was introduced previously to approximate the nullcline of MP in the FitzHugh-Nagumo model [36]. In the limit of $\tau \to 0$, the linear response of that system was obtained [37]. Here we obtain the linear dynamical response analytically for a one-dimensional bistable system with general τ.

The network up state exhibits properties significantly different from those in the down state, such as high irregularity [11,38], oscillatory activity with frequency located within β and γ ranges [39,40], and self-organized criticality [41]. Different mechanisms have been proposed to generate the network up and down states, including short-term depression in synaptic dynamics [41,42], and interaction between excitatory and inhibitory populations [11,43]. Bistability in individual neurons provides an alternative explanation for persistent activity in some brain areas [44,45], and is related to ramping neuronal activity implementing temporal information accumulation [46,47]. Our work sheds insights into the possible role of the up state on signal encoding and transmission through population response. Further work on building a network of interconnected such bistable units is needed to examine the relationship between the up state at the individual neuron level and at the circuit level [10,48].

ACKNOWLEDGMENTS

We thank J. Mejias, J. Murray, and F. Song for carefully reading the manuscript. This work was supported by a Swartz Foundation Fellowship (W.W.), grants from the Federal Ministry of Education and Research through the Bernstein Center for Computational Neuroscience Göttingen 01GQ1005B, 01GQ1005C (F.W.), and R01 MH062349 (X.-J.W.).

APPENDIX A: STATIONARY RESPONSE

When the mean input current μ and the noise strength σ are constants, the stationary response is obtained by setting the probability current to be constant, i.e., $J(\upsilon,t) = \nu_0$, where ν_0 is the stationary firing rate. Denote the stationary probability densities $P_0(\upsilon)$ within the left, middle, and right regions of the model as $P_{01}(\upsilon)$, $P_{03}(\upsilon)$, and $P_{02}(\upsilon)$, respectively. By utilizing the boundary conditions given in the main text, we have

$$\begin{aligned}
P_{01}(\upsilon) &= \frac{2\nu_0\tau}{\sigma}\, e^{-\frac{1}{\sigma^2}(\upsilon-\mu)^2} e^{A} \left(\frac{1}{\sqrt{r_1}} \int_{\frac{\tilde{\upsilon}_r+\mu}{\sqrt{r_1}\sigma}}^{\frac{\tilde{\upsilon}_1+\mu}{\sqrt{r_1}\sigma}} e^{-x^2}\, dx + \frac{1}{\sqrt{-r}} e^{B} \int_{\frac{\tilde{\upsilon}_b+\mu}{\sqrt{-r}\sigma}}^{\frac{\tilde{\upsilon}_1+\mu}{\sqrt{-r}\sigma}} e^{x^2}\, dx \right),\\
P_{03}(\upsilon) &= \frac{2\nu_0\tau}{\sigma}\, e^{\frac{1}{\sigma^2}(r_1(\upsilon-\upsilon_{t1})+\mu)^2} \left(\frac{1}{\sqrt{r_1}} \int_{\frac{r_1(\max(\upsilon,\upsilon_r)-\upsilon_{t1})+\mu}{\sqrt{r_1}\sigma}}^{\frac{\tilde{\upsilon}_1+\mu}{\sqrt{r_1}\sigma}} e^{-x^2} dx + \frac{1}{\sqrt{-r}} e^{B} \int_{\frac{\tilde{\upsilon}_b+\mu}{\sqrt{-r}\sigma}}^{\frac{\tilde{\upsilon}_1+\mu}{\sqrt{-r}\sigma}} e^{x^2}\, dx \right),\\
P_{02}(\upsilon) &= \frac{2\nu_0\tau}{\sqrt{-r}\sigma}\, e^{\frac{1}{r\sigma^2}(r(\upsilon-\upsilon_{t0})+\mu)^2} \int_{\frac{\tilde{\upsilon}_b+\mu}{\sqrt{-r}\sigma}}^{\frac{r(\upsilon-\upsilon_{t0})+\mu}{\sqrt{-r}\sigma}} e^{x^2} dx,
\end{aligned} \tag{A1}$$

where $\tilde{v}_1 = r_1(v_1 - v_{t1})$, $\tilde{v}_r = r_1(v_r - v_{t1})$, $\tilde{v}_b = r(v_b - v_{t0})$, $A = \frac{1}{\sigma^2}(1 + \frac{1}{r_1})(v_0 - \mu)^2$, and $B = \frac{1}{\sigma^2}(-\frac{1}{r_1} + \frac{1}{r})(\tilde{v}_1 + \mu)^2$. The stationary firing rate ν_0 is obtained from the normalization condition $\int_{-\infty}^{v_b} P_0(v)dv = 1$, which reads

$$\nu_0^{-1} = \tau_r + 2\tau\Bigg[e^A \int_{-\infty}^{\frac{v_0-\mu}{\sigma}} e^{-x^2}\,dx\left(\frac{1}{\sqrt{r_1}}\int_{\frac{\tilde{v}_r+\mu}{\sqrt{r_1}\sigma}}^{\frac{\tilde{v}_1+\mu}{\sqrt{r_1}\sigma}} e^{-x^2}\,dx + \frac{1}{\sqrt{-r}}e^B \int_{\frac{\tilde{v}_b+\mu}{\sqrt{-r}\sigma}}^{\frac{\tilde{v}_1+\mu}{\sqrt{-r}\sigma}} e^{x^2}\,dx\right) + \frac{1}{r_1}\int_{\frac{\tilde{v}_r+\mu}{\sqrt{r_1}\sigma}}^{\frac{\tilde{v}_1+\mu}{\sqrt{r_1}\sigma}} e^{-y^2}\,dy \int_{\frac{-v_0+\mu}{\sqrt{r_1}\sigma}}^{y} e^{x^2}\,dx$$
$$- \frac{1}{r}\int_{\frac{\tilde{v}_b+\mu}{\sqrt{-r}\sigma}}^{\frac{\tilde{v}_1+\mu}{\sqrt{-r}\sigma}} e^{-y^2}\,dy \int_{\frac{\tilde{v}_b+\mu}{\sqrt{-r}\sigma}}^{y} e^{x^2}\,dx + \frac{1}{\sqrt{-rr_1}}e^B \int_{\frac{-v_0+\mu}{\sqrt{r_1}\sigma}}^{\frac{\tilde{v}_1+\mu}{\sqrt{r_1}\sigma}} e^{x^2}\,dx \int_{\frac{\tilde{v}_b+\mu}{\sqrt{-r}\sigma}}^{\frac{\tilde{v}_1+\mu}{\sqrt{-r}\sigma}} e^{x^2}\,dx\Bigg]. \tag{A2}$$

APPENDIX B: PARABOLIC CYLINDER FUNCTIONS IN THE EXPRESSION OF LINEAR DYNAMICAL RESPONSE

Parabolic cylinder functions and their combinations are used in the expression of linear dynamical response. Parabolic cylinder functions $U(a,x)$ and $V(a,x)$ are two independent solutions of the Weber's equation

$$\frac{d^2y}{dx^2} - \left(\frac{1}{4}x^2 + a\right)y = 0\,,$$

and are normalized to satisfy $U'(a,x)V(a,x) - U(a,x)V'(a,x) = -\sqrt{\frac{2}{\pi}}$, where the prime represents derivative with respect to x [31].

The following parabolic cylinder functions are used in the linear dynamical response:

$$\psi_1(v) = U\left(-i\omega - \frac{1}{2}, -\frac{v-\mu}{\sqrt{D}}\right),$$
$$\Phi_1(v) = U\left(-i\omega + \frac{1}{2}, -\frac{v-\mu}{\sqrt{D}}\right),$$
$$\psi_2(v) = \sqrt{\frac{\pi D}{2}}V\left(-i\omega - \frac{1}{2}, -\frac{v-\mu}{\sqrt{D}}\right),$$
$$\psi_3(v) = U\left(-\frac{i\omega}{|r|} - \frac{1}{2}, -\frac{v - v_{t0} + \mu/r}{\sqrt{D/|r|}}\right),$$
$$\Phi_3(v) = U\left(-\frac{i\omega}{|r|} + \frac{1}{2}, -\frac{v - v_{t0} + \mu/r}{\sqrt{D/|r|}}\right),$$
$$\psi_4(v) = \sqrt{\frac{\pi D}{2|r|}}V\left(-\frac{i\omega}{|r|} - \frac{1}{2}, -\frac{v - v_{t0} + \mu/r}{\sqrt{D/|r|}}\right),$$
$$\Phi_4(v) = \sqrt{\frac{\pi D}{2|r|}}V\left(-\frac{i\omega}{|r|} + \frac{1}{2}, -\frac{v - v_{t0} + \mu/r}{\sqrt{D/|r|}}\right),$$
$$\psi_5(v) = U\left(-\frac{i\omega}{r_1} + \frac{1}{2}, -\frac{v - v_{t1} + \mu/r_1}{\sqrt{D/r_1}}\right),$$
$$\Phi_5(v) = U\left(-\frac{i\omega}{r_1} - \frac{1}{2}, -\frac{v - v_{t1} + \mu/r_1}{\sqrt{D/r_1}}\right),$$
$$\psi_6(v) = \sqrt{\frac{\pi D}{2r_1}}V\left(-\frac{i\omega}{r_1} + \frac{1}{2}, -\frac{v - v_{t1} + \mu/r_1}{\sqrt{D/r_1}}\right),$$
$$\Phi_6(v) = \sqrt{\frac{\pi D}{2r_1}}V\left(-\frac{i\omega}{r_1} - \frac{1}{2}, -\frac{v - v_{t1} + \mu/r_1}{\sqrt{D/r_1}}\right).$$

To simplify the expression, we use the following combinations of parabolic cylinder functions:

$$Y_1(v) = \psi_3(v)\psi_4(v_b) - \psi_4(v)\psi_3(v_b),$$
$$Y_2(v) = \psi_3(v)\Phi_4(v_b) + i\omega/r\ \psi_4(v)\Phi_3(v_b),$$
$$Y_5(v) = \psi_5(v_1)\psi_6(v) - \psi_6(v_1)\psi_5(v),$$
$$Y_6(v) = \psi_5'(v_1)\psi_6(v) - \psi_6'(v_1)\psi_5(v),$$
$$Y_{51}(v) = \psi_6(v)\Phi_5(v_1) - i\omega/r_1\psi_5(v)\Phi_6(v_1),$$
$$Y_{5r}(v) = \psi_5(v_r)\psi_6(v) - \psi_6(v_r)\psi_5(v),$$
$$Y_{51r}(v) = \psi_6(v)\Phi_5(v_r) - i\omega/r_1\psi_5(v)\Phi_6(v_r),$$
$$\begin{aligned} B = {} & (\psi_1'(v_0)Y_{5r}(v_0) - \psi_1(v_0)Y_{5r}'(v_0))e^{\Delta_0 + i\omega\tau_r} \\ & + ((\psi_1(v_0)Y_5'(v_0) - \psi_1'(v_0)Y_5(v_0))Y_1'(v_0) \\ & - (\psi_1(v_0)Y_6'(v_0) - \psi_1'(v_0)Y_6(v_0))Y_1(v_0))e^{\Delta_2}, \end{aligned}$$

where

$$\Delta_0 = \frac{1}{4D}(v_0 - v_r)(\tilde{v}_0 + \tilde{v}_r),$$
$$\Delta_1 = \frac{1}{4D}(v_0 - v_1)(\tilde{v}_0 + \tilde{v}_1),$$
$$\Delta_2 = \frac{1}{4D}[(v_0 - v_1)(\tilde{v}_0 + \tilde{v}_1) + (v_1 - v_b)(\tilde{v}_1 + \tilde{v}_b)].$$

Note that $\psi_2(v)$ is used in the derivation of the linear dynamical response, but does not appear in the final expression.

APPENDIX C: LINEAR DYNAMICAL RESPONSE IN A BISTABLE NEURON MODEL WITH BIOPHYSICALLY REALISTIC MEMBRANE CURRENTS

We check the linear dynamical response in a biologically realistic neuron model with up and down states stabilized by potassium currents. The neuronal dynamics has the following form:

$$\begin{aligned} \tau\frac{dV}{dt} = {} & -(V - V_L) - g_{AR}h_\infty(V - V_K) \\ & - g_{KS}m(V - V_K) + \mu_0 + \mu_{\text{ext}} + \sigma\eta(t), \end{aligned} \tag{C1}$$

where τ is a time constant determined by the leak conductance g_L. Normalized conductances for potassium currents, $g_{AR} \equiv \bar{g}_{AR}/g_L$ and $g_{KS} \equiv \bar{g}_{KS}/g_L$, are responsible for the down and up states, respectively. The first term in the right-hand side of Eq. (C1) is the leak current, the second term is an anomalously rectified potassium current that stabilizes the down state, and the third term is a non-inactivating potassium current which stabilizes the up state [11]. The voltage-dependent inactivation variable h_∞ is given by $h_\infty = \frac{1}{1+\exp[(V+90)/10]}$. The activation variable m satisfies

$$\frac{dm}{dt} = \frac{1}{\tau_\infty}(m - m_\infty) ,$$

where

$$m_\infty = \frac{1}{1+\exp[-(V+49)/3]} ,$$
$$\tau_\infty = \frac{10}{\exp[-(V+55)/30]+\exp[(V+55)/30]} .$$

The parameters used are: $\tau = 10$ ms, $V_L = -60$ mV, $V_K = -90$ mV, $g_{AR} = 50$, $g_{KS} = 5$, $V_r = -60$ mV, $V_b = -50$ mV, $\mu_0 = 100$ mV, $\mu_{\rm ext} = 0$, $\sigma = 10$ mV.

In Fig. 4 the linear dynamical response of this model is presented. The numerical results are obtained using the second-order Runge-Kutta method for stochastic differential equations [49]. When g_{KS} increases from 0 to 5, bistability is developed at the nullcline of the activation variable m, i.e., $m = m_\infty$ [Fig. 4(a)], and the model neuron exhibits up and down states [Fig. 4(b)]. We see that the normalized transmission function is significantly enhanced with the development of the up state [Fig. 4(c)].

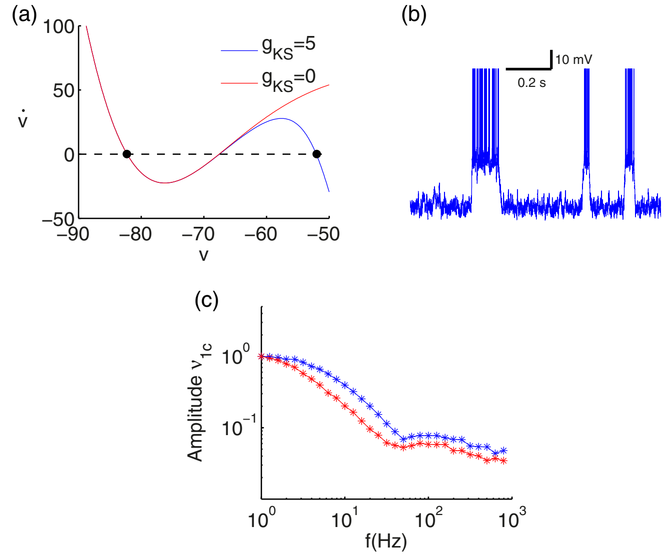

FIG. 4. (Color online) Impact of bistability on linear dynamical response in a biophysical realistic model. (a): membrane dynamics on the nullcline of activation variable m ($m = m_\infty$) with $g_{KS} = 0$ and 5. Here $\dot{V}$ in the vertical axis is the time derivative of V obtained by taking $\mu_{\rm ext} = 0$ and $\sigma = 0$ in Eq. (C1). (b): trajectory of membrane potential for $g_{KS} = 5$ and $\sigma = 10$ mV. (c): normalized transmission functions for the two different g_{KS}. Note that $\mu_{\rm ext}$ is reduced to -4 mV when $g_{KS} = 0$ to have similar stationary firing rates in the two cases (about 10 Hz).

[1] R. Llinas and M. Sugimori, Electrophysiological properties of in vitro Purkinje cell dendrites in mammalian cerebellar slices, J. Phys. (London) **305**, 171 (1980).
[2] C. Wilson and Y. Kawaguchi, The origins of two-state spontaneous membrane potential fluctuations of neostriatal spiny neurons, J. Neurosci. **16**, 2397 (1996).
[3] R. Lee and C. Heckman, Bistability in spinal motoneurons in vivo: Systematic variations in persistent inward currents, J. Neurophysiol. **80**, 583 (1998).
[4] I. Lampl, I. Reichova, and D. Ferster, Synchronous membrane potential fluctuations in neurons of the cat visual cortex, Neuron **22**, 361 (1999).
[5] J. Anderson, I. Lampl, I. Reichova, M. Carandini, and D. Ferster, Stimulus dependence of two-state fluctuations of membrane potential in cat visual cortex, Nat. Neurosci. **3**, 617 (2000).
[6] M. V. Sanchez-Vives and D. A. McCormick, Cellular and network mechanisms of rhythmic recurrent activity in neocortex, Nat. Neurosci. **3**, 1027 (2000).
[7] P. Heyward, M. Ennis, A. Keller, and M. T. Shipley, Membrane bistability in olfactory bulb mitral cells, J. Neurosci. **21**, 5311 (2001).
[8] S. R. Williams, S. R. Christensen, G. J. Stuart, and M. Häusser, Membrane potential bistability is controlled by the hyperpolarization-activated current I(H) in rat cerebellar Purkinje neurons in vitro, J. Phys. (London) **539**, 469 (2002).
[9] Y. Loewenstein *et al.*, Bistability of cerebellar Purkinje cells modulated by sensory stimulation, Nat. Neurosci. **8**, 202 (2005).
[10] N. Parga and L. F. Abbott, Network model of spontaneous activity exhibiting synchronous transitions between up and down states, Front. Neurosci. **1**, 57 (2007).
[11] A. Compte, M. V. Sanchez-Vives, D. A. McCormick, and X.-J. Wang, Cellular and network mechanisms of slow oscillatory activity (<1 Hz) and wave propagations in a cortical network model, J. Neurophysiol. **89**, 2707 (2003).
[12] M. Shadlen and W. Newsome, The variable discharge of cortical neurons: Implications for connectivity, computation, and information coding, J. Neurosci. **18**, 3870 (1998).
[13] B. Knight, The relationship between the firing rate of a single neuron and the level of activity in a population of neurons, J. Gen. Physiol. **59**, 767 (1972).
[14] W. Gerstner, Population dynamics of spiking neurons: Fast transients, asynchronous states, and locking, Neural Comput. **12**, 43 (2000).
[15] H. Köndgen, C. Geisler, S. Fusi, X.-J. Wang, H. R. Lüscher, and M. Giugliano, The dynamical response properties of neocortical neurons to temporally modulated noisy inputs in vitro, Cereb. Cortex **18**, 2086 (2008).
[16] C. Boucsein, T. Tetzlaff, R. Meier, A. Aertsen, and B. Naundorf, Dynamical response properties of neocortical neuron ensembles: Multiplicative versus additive noise, J. Neurosci. **29**, 1006 (2009).
[17] M. Higgs and W. Spain, Conditional bursting enhances resonant firing in neocortical layer 2-3 pyramidal neurons, J. Neurosci. **29**, 1285 (2009).

[18] T. Tchumatchenko, A. Malyshev, F. Wolf, and M. Volgushev, Ultrafast population encoding by cortical neurons, J. Neurosci. **31**, 12171 (2011).
[19] V. Ilin, A. Malyshev, F. Wolf, and M. Volgushev, Fast computations in cortical ensembles require rapid initiation of action potentials, J. Neurosci. **33**, 2281 (2013).
[20] N. Brunel, F. S. Chance, N. Fourcaud, and L. F. Abbott, Effects of Synaptic Noise and Filtering on the Frequency Response of Spiking Neurons, Phys. Rev. Lett. **86**, 2186 (2001).
[21] B. Lindner and L. Schimansky-Geier, Transmission of Noise Coded Versus Additive Signals Through a Neuronal Ensemble, Phys. Rev. Lett. **86**, 2934 (2001).
[22] W. Wei and F. Wolf, Spike Onset Dynamics and Response Speed in Neuronal Populations, Phys. Rev. Lett. **106**, 088102 (2011).
[23] N. Fourcaud-Trocmè, D. Hansel, C. van Vreeswijk, and N. Brunel, How spike generation mechanisms determine the neuronal response to fluctuating inputs, J. Neurosci. **23**, 11628 (2003).
[24] N. Fourcaud-Trocmè and N. Brunel, Dynamics of the instantaneous firing rate in response to changes in input statistics, J. Comput. Neurosci. **18**, 311 (2005).
[25] C. Geisler, N. Brunel, and X.-J. Wang, Contributions of intrinsic membrane dynamics to fast network oscillations with irregular neuronal discharges, J. Neurophysiol. **94**, 4344 (2005).
[26] B. Naundorf, T. Geisel, and F. Wolf, Action potential onset dynamics and the response speed of neuronal populations, J. Comput. Neurosci. **18**, 297 (2005).
[27] M. J. E. Richardson, Firing-rate response of linear and nonlinear integrate-and-fire neurons to modulated current-based and conductance-based synaptic drive, Phys. Rev. E **76**, 021919 (2007).
[28] I. Timofeev, F. Grenier, and M. Steriade, Disfacilitation and active inhibition in the neocortex during the natural sleep-wake cycle: An intracellular study, Proc. Natl. Acad. Sci. USA **98**, 1924 (2001).
[29] C. van Vreeswijk and H. Sompolinsky, Chaos in neuronal networks with balanced excitatory and inhibitory activity, Science **274**, 1724 (1996).
[30] H. Risken, *The Fokker Planck Equation: Methods of Solution and Applications* (Springer-Verlag, Berlin, 1984).
[31] M. Abramowitz and I. A. Stegun, *Tables of Mathematical Functions* (Dover Publications, New York, 1970).
[32] X.-J. Wang, Neurophysiological and computational principles of cortical rhythms in cognition, Physiol. Rev. **90**, 1195 (2010).
[33] G. Buzsáki and X.-J. Wang, Mechanisms of gamma oscillations, Annu. Rev. Neurosci. **35**, 203 (2012).
[34] G. Buzsáki and E. Schomburg, What does gamma coherence tell us about inter-regional neural communication? Nat. Neurosci. **18**, 484 (2015).
[35] S. Cogno, S. Schreiber, and I. Samengo, Dynamics and reliability of bistable neurons driven with time-dependent stimuli, Neural Comput. **26**, 2798 (2014).
[36] H. McKean, Nagumo's equation, Adv. Math. **4**, 209 (1970).
[37] B. Lindner and L. Schimansky-Geier, Coherence and stochastic resonance in a two-state system, Phys. Rev. E **61**, 6103 (2000).
[38] J. F. Mejias, H. J. Kappen, and J. J. Torres, Irregular dynamics in up and down cortical states, PLoS ONE **5**, e13651 (2010).
[39] A. Compte, R. Reig, V. F. Descalzo, M. A. Harvey, G. D. Puccini, and M. V. Sanchez-Vives, Spontaneous high-frequency (10–80 Hz) oscillations during up states in the cerebral cortex in vitro, J. Neurosci. **28**, 13828 (2008).
[40] J. Hidalgo, L. F. Seoane, J. M. Cortès, and M. A. Munoz, Stochastic amplification of fluctuations in cortical up-states, PLoS ONE **7**, e40710 (2012).
[41] D. Millman, S. Mihalas, A. Kirkwood, and E. Niebur, Self-organized criticality occurs in non-conservative neuronal networks during up states, Nat. Phys. **6**, 801 (2010).
[42] D. Holcman and M. Tsodyks, The emergence of up and down states in cortical networks, PLoS Comput. Biol. **2**, e23 (2006).
[43] M. Bazhenov, I. Timofeev, M. Steriade, and T. Sejnowski, Model of thalamocortical slow-wave sleep oscillations and transitions to activated states, J. Neurosci. **22**, 8691 (2002).
[44] E. Marder, L. F. Abbott, G. G. Turrigiano, Z. Liu, and J. Golowasch, Memory from the dynamics of intrinsic membrane currents, Proc. Natl. Acad. Sci. USA **93**, 13481 (1996).
[45] M. Camperi and X.-J. Wang, A model of visuospatial working memory in prefrontal cortex: Recurrent network and cellular bistability, J. Comput. Neurosci. **5**, 383 (1998).
[46] H. Okamoto and T. Fukai, Recurrent network models for perfect temporal integration of fluctuating correlated inputs, PLoS Comput. Biol. **5**, e1000404 (2009).
[47] K. W. Latimer, J. L. Yates, M. L. Meister, A. C. Huk, and J. W. Pillow, Single-trial spike trains in parietal cortex reveal discrete steps during decision-making, Science **349**, 184 (2015).
[48] M. Stern, H. Sompolinsky, and L. F. Abbott, Dynamics of random neural networks with bistable units, Phys. Rev. E **90**, 062710 (2014).
[49] R. L. Honeycutt, Stochastic Runge-Kutta algorithms. I. White noise, Phys. Rev. A **45**, 600 (1992).